JOURNAL OF MAPS
2025, VOL. 21, NO. 1, 2465669
https://doi.org/10.1080/17445647.2025.2465669

SCIENCE

OPEN ACCESS Check for updates

Global distribution of canali on Venus

Sydney A. Bledsoe and Christian Klimczak

Center for Planetary Tectonics at UGA, Department of Geology, University of Georgia, Athens, GA, USA

ABSTRACT

The surface of Venus shows an abundance of channels with constant widths along their lengths and a simple channel structure that are interpreted to have formed volcanically. They have the International Astronomical Union (IAU) descriptor term 'vallis, valles'. Previous research focused heavily on the 7400-km-long Baltis Vallis but there is no systematic map documenting the total extent of all 72 named channels. Here, we systematically mapped 66 of the channels that could be clearly identified in NASA's Magellan SAR data. From our map, we compiled physical characteristics including length, sinuosity, and channel orientation. Lengths range from 70 to 7400 km, their sinuosities fall between 1.03 and 2.25, and we detect no global trend in preferred orientation or flow direction. Our map improves the global geologic map products available for Venus and, as highlighted for Ikhwezi Vallis, is useful for a detailed interpretation of the geologic history of our second planet.

ARTICLE HISTORY
Received 11 November 2024
Revised 3 February 2025
Accepted 5 February 2025

KEYWORDS
Volcanism; Venus; Tectonics

1. Introduction

Around 80% of the surface of Venus is shaped by volcanic activity, including plains volcanism, lava flows, and lava channels (Basilevsky & Head, 2003; Ford et al., 1993; Head et al., 1992; Ivanov & Head, 2011). Understanding volcanism on Venus is thus vital to its geologic history. The surface of Venus is known to be geologically young (Basilevsky & Head, 2003), which has traditionally been debated in the literature to be the result of either rapid lithospheric overturn (Schaber et al., 1992; Strom et al., 1994; Turcotte, 1993) or gradual resurfacing (Phillips et al., 1992; Smrekar et al., 2010).

Among the volcanic landforms observed globally across Venus are long, sinuous channels that were assigned the International Astronomical Union (IAU) descriptor term 'vallis, valles' (Baker et al., 1992; Komatsu et al., 1992). These channels have lengths up to several thousand kilometers and along their length have constant widths that average 3–5 km (Baker et al., 1997). In cross-section these channels are shown to have floors that are 20–100 m lower than the surrounding terrain, with the presence of levees first noticed along Baltis Vallis that point to an erosional origin (Oshigami & Namiki, 2007). Additionally, the presence of delta-like debouchments, detached sinuous parts of channels akin to cut-off meanders, and other characteristics seen in terrestrial fluvial morphology all also point to formation by erosional rather than constructional processes (Bray et al., 2007; Bussey et al., 1995). The volcanic origin of these channels has been investigated with thermodynamic modeling and simulations, showing that carbonatitic, sulfuric, or other exotic lava compositions are capable of flowing for the observed, long distances without solidifying that require for erosion to be mechanical as opposed to thermal (Bussey et al., 1995; Gregg & Greeley, 1993; Komatsu et al., 1992; Williams-Jones et al., 1998). Other interpretations of these channels include formation by subsurface flow or them being of aqueous origin (Jones & Pickering, 2003; Lang & Hansen, 2006).

This type of channel structure is not unique to Venus. Similar landforms have been reported from the Moon where they are referred to as sinuous rilles (Hurwitz et al., 2013b), from Mars (Hopper & Leverington, 2014; Jaeger et al., 2007), and also Mercury (Hurwitz et al., 2013a). While there is consensus for the channels on the Moon and Mercury to be of volcanic origin (Byrne et al., 2013; Hurwitz et al., 2012), the majority of channels on Mars are currently interpreted to be fluvial in origin (Group, 1983) with some evaluated as volcanic (Hopper & Leverington, 2014; Jaeger et al., 2007). On Venus, these channels are likely formed by a low viscosity lava (Bray et al., 2007; Komatsu et al., 1992; Williams-Jones et al., 1998). The channels on Venus stand out as they are unusually long. The longest of them, Baltis Vallis,

CONTACT Sydney A. Bledsoe sb57621@uga.edu Center for Planetary Tectonics at UGA, Department of Geology, University of Georgia, 210 Field Street, Athens, GA 30602, USA

Supplemental map for this article is available online at https://doi.org/10.1080/17445647.2025.2465669

was previously reported to show a length in excess of 6800 km, which is longer than the Nile River and thus is the longest channelized flow of any kind known in our solar system (Oshigami & Namiki, 2007). Several other channels are also thousands of kilometers in length (Baker et al., 1992), attesting to their importance for understanding volcanism on the second planet. Despite the previous work and there being 72 named channels on Venus, there is no global map and study specifically addressing the distribution and characteristics of the entire population of channels, motivating the research in this work.

In addition to the global geologic map by Ivanov and Head (2011), there are many regional quadrangle geologic maps of Venus (e.g. Lang & Hansen, 2010). We use the map by Ivanov and Head (2011) because it allows us to compare the distribution of units with respect to our mapping consistently across Venus. Future observations made on other geologic maps will be possible using our mapping. The units defined by Ivanov and Head (2011) include tesserae, densely lineated plains, ridged plains, mountain belts, groove belts, shield plains, regional plains, shield clusters, smooth plains, lobate plains, and rift zones (Ivanov & Head, 2011). In addition to the surface geology, the map includes the locations of other prominent landforms, such as coronae mapped as polygons, craters mapped as points, and channels mapped as polylines. Even though the global map by Ivanov and Head (2011) contains channels as a mapped feature class, the linework does not capture the detail that is apparent in the available image data. For example, many channels remain unmapped, and those that are mapped lack detail, such that a straight polyline marks the channel location but does not capture the true pathway and length of the channel. Therefore, we systematically map all named channels on Venus that could be clearly identified in the present data and discuss global and local implications for the geology of Venus.

2. Methods

To identify lava channels on Venus, we used the synthetic aperture radar (SAR) image mosaics from the NASA Magellan spacecraft that orbited Venus from 1989 to 1994. The SAR had a wavelength of 12.6 cm, which is S-band at 2.385 GHz (Ford et al., 1993). The SAR mosaics combine images from two different cycles and look angles, where cycle 1 is left-look, or eastward, and cycle 2 is right-look, or westward. The majority of the data for this mosaic was gathered during cycle 1 whereas imaging in cycle 2 focused on filling in the gaps, together resulting in a global coverage of 99% at a resolution of 75 m per pixel (Ford et al., 1993; Saunders et al., 1992). For the mapping, we loaded the SAR mosaics into a GIS using ArcGIS 10.8. Into that same GIS, we added the IAU Gazetteer of Planetary Nomenclature shapefile that contains all named features on Venus including 72 valles, which is provided open access by the United States Geological Survey (IAU and USGS, 2012, sec. Venus). We note that there are more channels that fit the definition of 'vallis' on Venus than those 72 named by the IAU, as documented by López et al. (2023). The named channels are the longest, best defined structures, whereas any unnamed channels are short. In this mapping effort, we focus on the named channels, as their locations are well known. Future mapping will include a survey of additional, unnamed channels.

We located every landform designated as vallis and mapped them at a map scale of 1:125,000 in a stereographic projection. Using a stereographic projection minimized angle distortions close to the center of projection. We traced the channels as polylines using the streaming function with a tolerance of one vertex per 1000 map units, which resulted in equally spaced vertices every 1 km along the length of the channel. In order to maintain consistent vertex placement that may be needed for further analysis requiring consistent sampling of map data, we defined 10° by 10° geographic bins (Figure 1(a)). We then reprojected the map to the center of each geographic bin in which a channel was found and only mapped that portion of the channel that was located inside the bin (Figure 1(b)). The reprojection ensured that every segment was mapped no more than $5\sqrt{2}$ decimal degrees, or ~750 km, from the center of projection, resulting in minimal distortions of vertex spacing.

For our mapping, we closely follow the Guide to Magellan Image Interpretation (Ford et al., 1993). Generally, synthetic aperture radar measures the energy that is reflected back from the surface to the sensor, such that higher energy received is a brighter radar reading. Radar is scattered more on rough surfaces and thus more energy is reflected back to the sensor, while a smooth terrain will reflect energy away from the sensor. This relation means that radar bright regions in SAR can be interpreted to have a rough terrain and radar dark regions to be smooth terrain (Ford et al., 1993).

In particular, mapping channelized lava flows, the channel floor and walls appear in several combinations of bright and dark within the SAR mosaics (Baker et al., 1992). Most commonly, the channel floor was radar dark with channel walls that were indistinguishable from the surrounding terrain, but in places the walls were radar bright. In instances where the channel floor was the same brightness as the surrounding terrain, the walls were commonly radar bright, but in less common cases they may be radar dark. In the ideal case, two radar bright visible walls are seen (Figure 2(a)). Challenges in recognizing the channels include when only one channel wall is

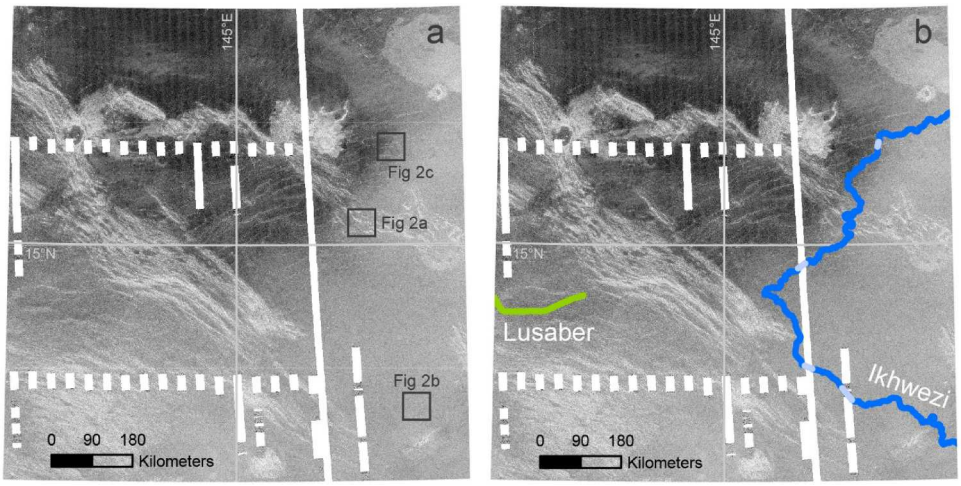

Figure 1. An example of a 10° by 10° study area used for mapping shown in a stereographic projection centered at 15°N, 145°E. (a) Coverage of the Magellan SAR left-look mosaic, where the white rectangles are data gaps (gores). (b) Ikhwezi and Lusaber Valles are channels shown in blue and green, respectively, that were mapped with a polyline in this area. The light blue segments represent inferred sections of Ikhwezi Vallis at gores.

visible (Figure 2(b)), parts of the channel are covered by lava flows or faulting (Figure 2(c)), or where the SAR mosaic is too noisy to distinguish a channel from the surrounding terrain.

When both channel walls were visible in the SAR data and/or when the channel floor was clearly distinct from the surrounding terrain, then the polyline was placed between them, tracing the channel floor. When only one channel wall was visible in the SAR images and the channel floor was indistinguishable from the surrounding terrain, then the polyline was mapped along that wall. We encountered many cases where a channel passed through a data gap, or gore, in the SAR mosaics, and no visual information was available. In these cases, the polyline ends at the gore and is resumed on the other side. A straight polyline was used to connect the two ends when it was reasonable to assume the channel continued throughout the gore, which helped us to calculate the total length of the channels (Figure 1(b)). Several channels have been superposed or were rendered unrecognizable by other geological phenomena, such as heavily fractured terrain (Figure 2(c)). In those cases, the same procedure as that for mapping across gores was followed, whereby channels that maintained the same characteristics on both sides, were connected with a straight polyline. We created different polylines for each of the 10° by 10° geographic bins and once a channel was fully mapped, we merged the polylines at their shared endpoints for a single map trace. Separate branches, small offshoots, and secondary channels were kept as separate polylines within the shapefile.

3. Results

Of the 72 named valles, we successfully located and mapped 66 of them (Figure 3) and cataloged physical information including length, sinuosity, and the primary orientation (Table 1). Channels generally have a global distribution (Figure 3(a)) but are mostly located in topographically low-lying areas (Figure 3(b)). We also note where secondary branches were mapped as separate polylines, whereby the primary, i.e. longer, channel is denoted with a (1) and the secondary, i.e. shorter, channel is denoted with a (2) within Table 1. The Main Map displays the location of channels with respect to Venus quadrangles. Additionally, we note where channels are part of a channel complex, a situation where several named channels connect, where channels occur in terrain other than lowland lava plains, or where channels with different names are likely part of the same landform.

We extracted the lengths of all mapped channels, showing that they vary in length from 70 to 7400 km, with 28 of them being longer than 500 km, and 9 of those exceeding a length of 1000 km (Table 1). To visualize the total range of channel lengths, we display the data in a box and whisker plot (Figure 4(a)). In the plot, the lower and upper whiskers are the minimum and maximum values, respectively. The thick black line in the center is defined by the median of the data, which splits the data into lower and higher quartiles. The bottom edge of the box marks the median of the lower data, while the upper edge of the box marks the median of the higher data. The longest channels are considered statistical outliers, they are shown as circles. The shortest channel is the 66-km-long Yuvkha Vallis, and the maximum length value designated by the upper whisker is represented by the 1286-km-long Gendenwitha Vallis. The median length of the channels is 462 km, coinciding with Fetu-ao Vallis. The median of the lower data is represented by the 258-km-long Albys Vallis, and that

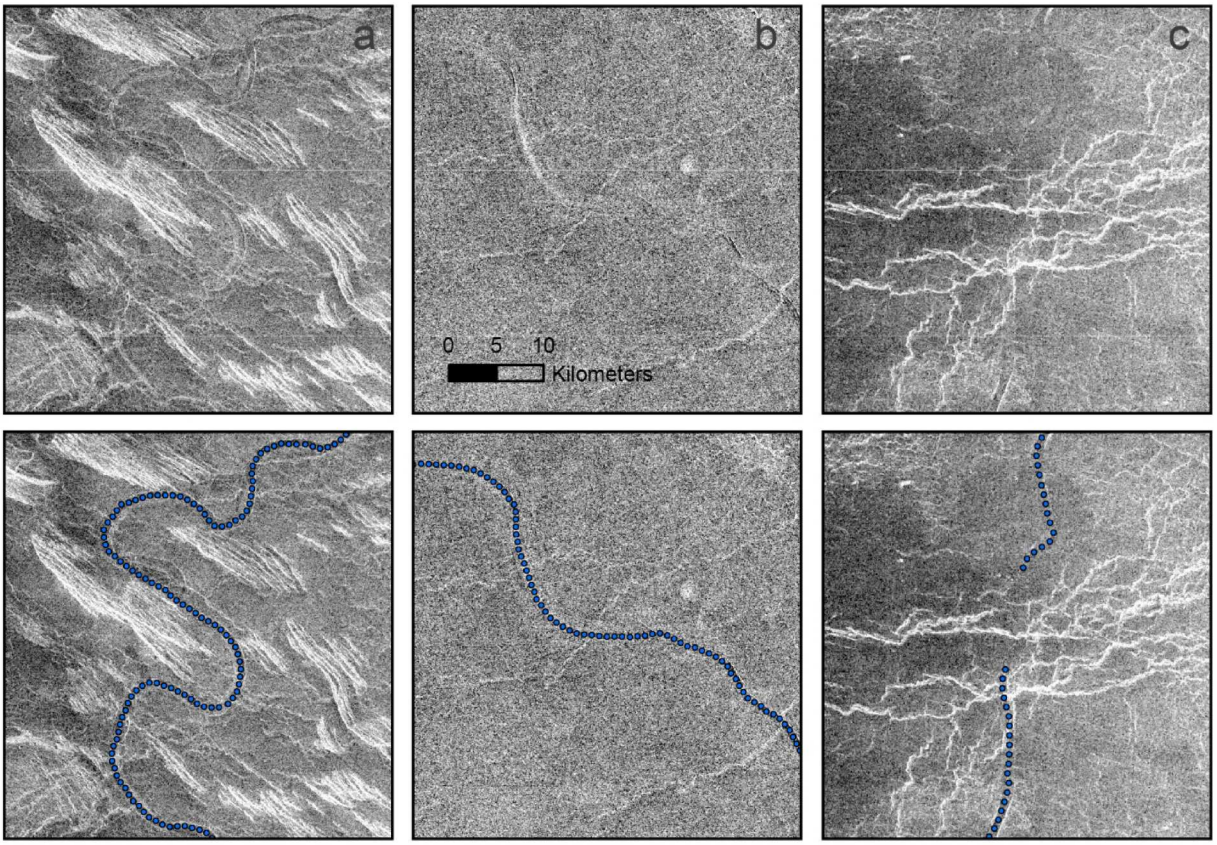

Figure 2. Channel characteristics of Ikhwezi Vallis in the Magellan SAR image mosaic. The top row shows a channel in the SAR mosaic image and the bottom row is the polyline vertices that we mapped. The location of these images is indicated in Figure 1(a), the scale applies to all images. (a) A noticeably sinuous portion of the channel is observed to be curving through a groove belt, which appears as radar bright densely lineated unit. Both channel walls are visible but the channel floor largely indistinguishable from the surrounding terrain, except in the northernmost portions of this image, where the channel floor is radar dark. (b) Example of our map trace, where both walls are not visible but the channel floor appears as radar bright and dark sinuous line. (c) Example of a channel that was rendered unrecognizable by fractures, which are seen as radar bright lineaments.

of the higher data is the 752-km-long Bennu Vallis. The longest channels are Ikhwezi Vallis (1919 km), Laidamlulum Vallis (2502 km), Citlalpul Vallis (3177 km), and Baltis Vallis (7431 km).

Next, we computed the sinuosity of the channel, which is defined as the ratio of the length of the channel over the straight-line distance between the channel endpoints. A perfectly straight channel has a ratio of 1, and channels with increasingly curvy, or sinuous, map traces will display ratios larger than 1. To visualize the total range of mapped channel sinuosities, we also visualize our results in a box and whisker plot (Figure 4(b)). Overall, the sinuosities range from 1.03 for both Nantosuelta and Hoku-ao Valles to 2.25 for Albys Vallis. Represented by the whiskers in the boxplot, the minimum and maximum values of 1.03 and 1.85 correspond to Hoku-ao or Nantosuelta Valles and Baltis Vallis, respectively. The median sinuosity coincides with Alajen Vallis having a value of 1.24. The bottom of the box that represents the median of the lower data is 1.15, which is the value for each Ta'urua, Uottakhsulus, Austrina, and Fetu-ao Valles, while the top of the box, represented by Gendenwitha Vallis, has a value of 1.45. The most sinuous channels, considered statistical outliers in the boxplots, are Ikhwezi Vallis (1.91), Kallistos Vallis (1.92), Dzyzlan Vallis (1.95), Xulab Vallis (2.05), and Albys Vallis (2.25).

We also visually extracted the primary orientations of the mapped channels. We list orientations of channels to indicate directionality of lava flows, as it was impossible to uniquely identify flow direction at any of the channels with our mapping. Flow direction can be determined by locating the channel source or terminus, seeing a distinct thinning towards the end as a result of material loss down length, or delta-like structures at one end similar to the terminus of terrestrial rivers (Baker et al., 1997; Williams-Jones et al., 1998). The overall channel structure can also be a clue, as lava channels may form distributary structures; however, lava channels may also form in tributary structures, where more than one indicator is needed to determine flow direction (Dietterich & Cashman, 2014). Because these indicators are either not present or not visible in the SAR mosaics, we report channel orientations instead. A total of 24 channels are oriented generally in north-south

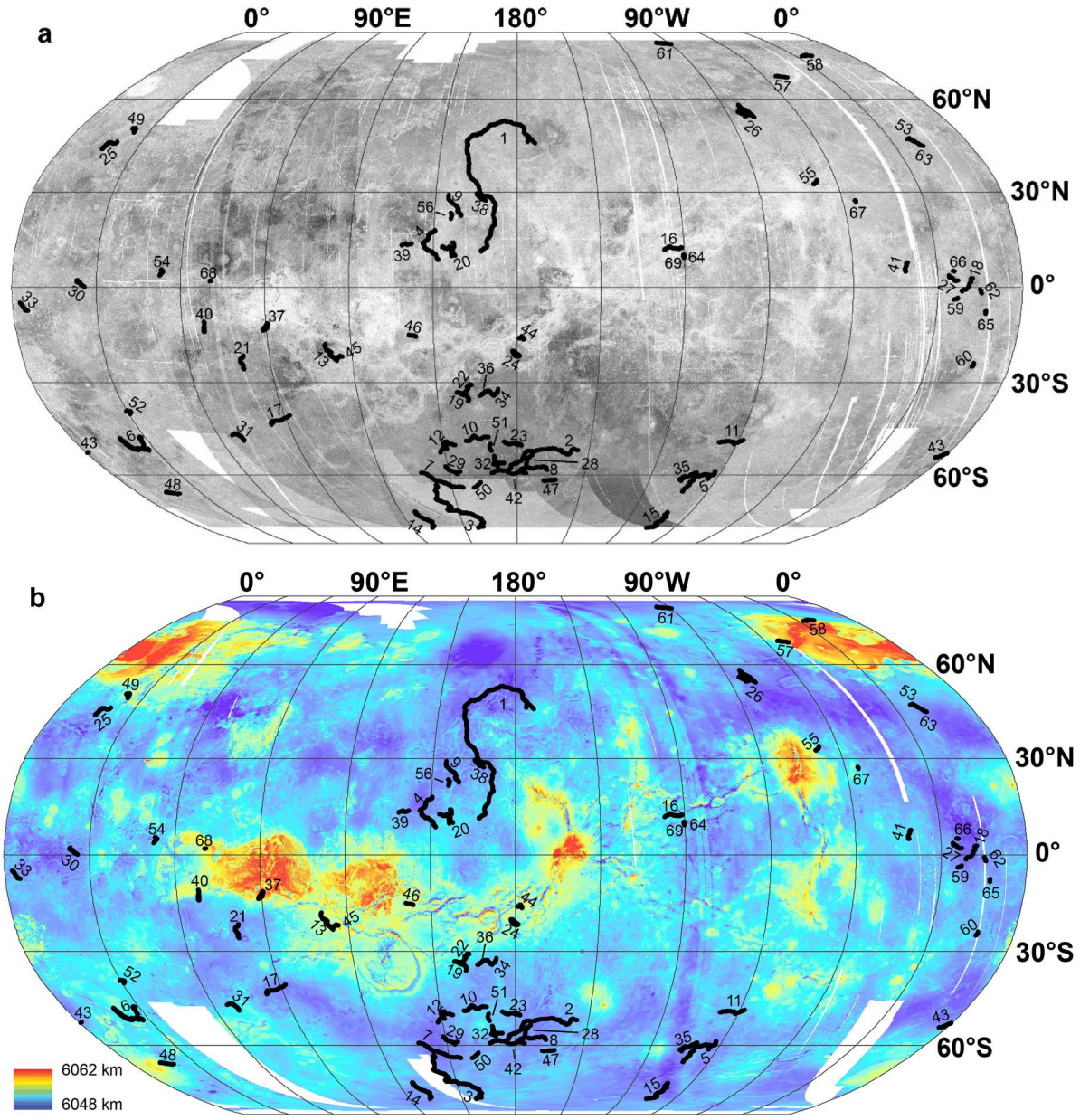

Figure 3. Global maps of Venus shown in Robinson projection centered on 180°, 0° overlain by our polyline shapefile of channels in black where the number labels of the channels correspond to those listed in Table 1. (a) Global map of channels on the combined Magellan SAR left-, and right-look mosaics. (b) Global map of channels shown with respect to Magellan global topography, where cool colors represent low-lying topography, and warm colors represent high-standing terrain.

directions, 17 channels are oriented generally in east-west directions, 15 channels are generally aligned northwest-southeast, and 13 channels are oriented northeast-southwest. These orientations show that there is no systematic directionality of lava flow discernable from the orientation of the channel.

Six of the 72 named valles could not be located within the Magellan SAR mosaic and thus are not part of the map. These channels are Kumanyefie, Ngyandu, Ymoja, Anuket, Sezibwa, and Nommo Valles. The marker for Kumanyefie Vallis lies near the south pole, which is not covered by the Magellan SAR mosaic. In the areas where Ngyandu, Ymoja, and Nommo Valles are marked to be, no structure resembling a channel is visible in the mosaic after thorough surveying the regions. At the marker for Anuket Vallis, the terrain is complicated, and we were not able to clearly discern a channel. Sezibwa Vallis is marked to be within a complex lava flow, but no distinct channel could be identified in this location.

4. Discussion and conclusions

We have mapped 66 lava channels globally (Figure 3) amounting to a length in excess of 45,000 km that can be added to any global geological map of Venus. We make our shapefile publicly available in Bledsoe and Klimczak (2024). For example, the global geological map by Ivanov and Head (2011) does not include these channels with the same detail, their total mapped channel length is half of that than ours only measuring ~23,000 km. In some cases, the channels in Ivanov

Table 1. Compilation of measurements and notes for all 72 named lava channels on Venus.

Map Number	Name	Length (km)	Sinuosity	Primary orientation	Notes
1	Baltis	7431	1.83	N/S	
2	Citlalpul	3177	1.36	NE/SW	In a complex with Xulab (8), Dilbat (28), and Vesper (42)
3	Laidamlulum	2502	1.37	N/S	Mapped in right-look, extends off of map so true length is longer than recorded
4	Ikhwezi	1919	1.91	N/S	
5	Gendenwitha	1286	1.45	NE/SW	
6	Kallistos	1254	1.92	E/W	Not all meanders mapped, lies within lobate plain
7	Sholpan	1112	1.09	NW/SE	Likely same channel as Merak (50)
8	Xulab	1079	2.05	E/W	In a complex with Citlalpul (2), Dilbat (28), and Vesper (42)
9	Jutrzenka	1032	1.23	NW/SE	
10	Lusaber	906	1.36	E/W	
11	Sinann	856	1.28	E/W	
12	Umaga	834	1.65	NE/SW	Mapped in right-look
13	Morongo (1)	826	1.27	NW/SE	Interpreted primary (13) and secondary (45) channel system, mapped in right-look, lies in lobate plains
14	Koidutäht	810	1.11	N/S	Mapped in right-look, extends off of map so true length is longer than recorded
15	Ta'urua	805	1.15	N/S	Mapped in right-look, extends off of map so true length is longer than recorded
16	Uottakh-sulus	765	1.15	E/W	Lies in lobate plains
17	Tan-yondozo	760	1.12	NE/SW	
18	Bennu	752	1.23	NE/SW	
19	Vishera (1)	751	1.59	NW/SE	Interpreted primary (19) and secondary (22) channel system, mapped in right-look
20	Tai-Pe	729	1.54	N/S	
21	Ahsabkab	670	1.46	N/S	Mapped in right-look
22	Vishera (2)	628	1.36	NE/SW	Interpreted primary (19) and secondary (22) channel system, mapped in right-look
23	Austrina	589	1.15	E/W	
24	Poranica	588	1.81	NW/SE	Lies in lobate plains
25	Bayara	580	1.53	NE/SW	
26	Utrenitsa	565	1.40	N/S	Complicated, semi-radial branches
27	Sati	518	1.36	NW/SE	
28	Dilbat	510	1.11	N/S	In a complex with Citlalpul (2), Xulab (8), and Vesper (42)
29	Kümsong	493	1.26	N/S	
30	Nepra	489	1.31	NW/SE	
31	Kimtinh	485	1.52	NW/SE	Mapped in right-look
32	Nahid	484	1.36	N/S	
33	Banumbirr	478	1.22	NW/SE	Lies in shield plains, and interaction with crater at southern end
34	Helmud	474	1.73	NE/SW	Likely same channel as Matlalcue (36), mapped in right-look
35	Fetu-ao	462	1.15	NW/SE	
36	Matlalcue	447	1.18	NE/SW	Likely same channel as Helmud (34), mapped in right-look
37	Lo Shen	427	1.56	N/S	Lies in smooth plains
38	Hoku-ao	419	1.03	NW/SE	In close proximity to Baltis (1)
39	Kinsei	417	1.10	E/W	Abnormal width of 10–12 km
40	Tawera	403	1.18	N/S	Lies in lobate plains
41	Tingoi	398	1.29	N/S	
42	Vesper	376	1.21	E/W	In a complex with Citlalpul (2), Xulab (8), and Dilbat (28)
43	Chasca	362	1.12	NE/SW	Lies in smooth plains
44	Dzyzlan	353	1.95	E/W	Mapped in right-look, lies in a rift zone
45	Morongo (2)	304	1.21	NE/SW	Interpreted primary (13) and secondary (45) channel system, mapped in right-look, lies in lobate plains
46	Veden-Ema	297	1.05	E/W	Lies in lobate plains and rift zone
47	Nantosuelta	293	1.03	E/W	
48	Apisuahts	292	1.17	E/W	Mapped with right-look, lies in lobate plains
49	Belisama	277	1.46	N/S	Lies in lobate plains
50	Merak	269	1.06	NE/SW	Likely same channel as Sholpan (7), mapped in right-look
51	Khalanasy	265	1.09	N/S	
52	Albys	258	2.25	NW/SE	Lies in lobate and shield plains
53	Nyakaio	257	1.21	NW/SE	Likely same channel as Fufei (63)
54	Ganga	256	1.36	N/S	Lies in shield plains
55	Omutnitsa	253	1.29	NE/SW	
56	Martuv	243	1.19	N/S	
57	Lunang	233	1.17	E/W	
58	Saga	215	1.49	E/W	Lies in the tesserae
59	Alajen	214	1.24	E/W	
60	Samundra	178	1.34	N/S	Abnormal width, large pool at one end
61	Olokun	173	1.19	NW/SE	
62	Fara	164	1.17	N/S	Lies in shield plains
63	Fufei	158	1.11	NW/SE	Likely same channel as Nyakaio (53)
64	Yuvkha (1)	119	1.22	N/S	Two visible channels (64) and (69), lies in rift zone and shield plain
65	Bastryk	112	1.18	N/S	
66	Vakarine	92	1.13	E/W	
67	Tapati	88	1.30	N/S	
68	Avfruvva	72	1.09	E/W	Lies in smooth plains, fault interaction

(*Continued*)

Table 1. Continued.

Map Number	Name	Length (km)	Sinuosity	Primary orientation	Notes
69	Yuvkha (2)	66	1.13	N/S	Two visible channels (64) and (69), lies in rift zone and shield plain
–	Kumanyefie	–	–	–	Could not be located
–	Ngyandu	–	–	–	Could not be located
–	Ymoja	–	–	–	Could not be located
–	Anuket	–	–	–	Could not be located
–	Sezibwa	–	–	–	Could not be located
–	Nommo	–	–	–	Could not be located

Note: Channels labeled with a number (1) or (2) are separate landforms as part of the same named vallis, and thus they were mapped as separate sections and measurements were computed separately. The channel number corresponds to the labels in Figure 3.

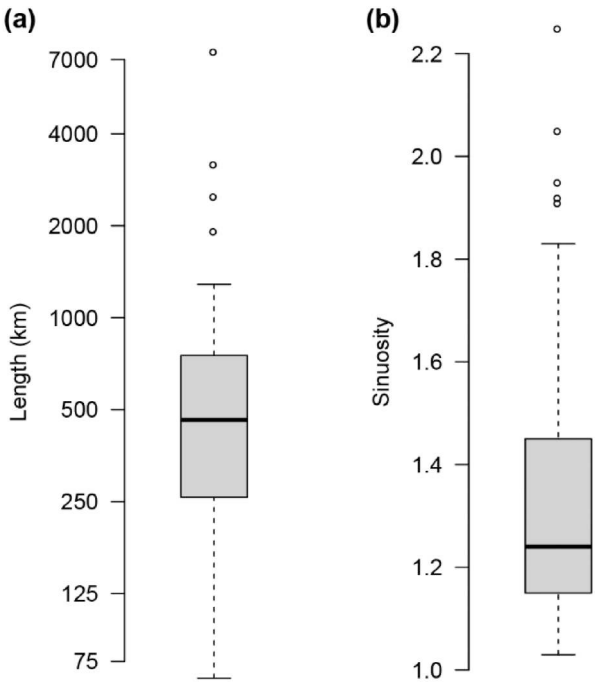

Figure 4. Box-and-whisker plot showing compiled length and sinuosity data for lava channels on Venus. The lower and upper whiskers are the minimum and maximum values, respectively. The thick black line is the median of the data, which splits the data into lower and higher quartiles. The bottom edge of the box is the median of the lower data, while the upper edge of the box is the median of the higher data. The circles are statistical outliers. (a) Plot illustrating the distribution of the extracted lengths of lava channels. (b) Boxplot showing the distribution of channel sinuosity.

and Head (2011) are short polylines marking that a channel is present, but these polylines do not capture the true channel pathway and do not include all discernable channels. The resulting map of this research can be used in conjunction with the geologic map by Ivanov and Head (2011) to gain a better understanding of global and regional volcanic processes, because they are widespread across the surface of Venus, occurring mostly in regional plains. Interestingly, they are also found in a series of other geologic units (Table 1). A total 48 lie in the regional plains that make up 80% of the surface of Venus. The remaining 18 channels that lie in other units are Kallistos, Morongo, Uottakh-sulus, Poranica, Banumbirr, Lo Shen, Tawera, Chasca, Dzyzlan, Veden-Ema, Apisuahts, Belisama, Albys, Ganga, Saga, Fara, Yuvkha, and Avfruvva Valles (Table 1). In each of their paths, the channels date as one of the youngest or *the* youngest landform.

Ikhwezi Vallis, in particular, demonstrates a series of geologic relationships that are possible to infer from detailed interpretation of the map relationships (Figure 5). We compare the channel path to the global geologic map by Ivanov and Head (2011) as an example. Other geologic interpretations exist, thus comparisons with our channel map may also be different using those other maps. In our example, the radar-dark channel floor can be followed in a sinuous path through deformed portions of a groove belt, defined as a heavily deformed structural unit comprised of extensional structures (Ivanov & Head, 2011), thus relatively dating Ikhwezi Vallis as younger than the groove belt. This relationship shows that during the active flow that formed Ikhwezi Vallis, the groove belt was a series of topographic highs between which channelized lava was able to flow through in the topographic lows. This relationship is locally consistent with previous research where the groove belts are thought to have formed before or concurrent with the plains volcanism (Ivanov & Head, 2011). Future in-depth analysis of relative ages and geologic relationships like the ones described along Ikhwezi Vallis, also including different geologic map interpretations, may be able to further specify stratigraphic relationships and thus place the channelized lava flows in a regional and global geologic context, as has been done for Baltis Vallis along its length (Basilevsky & Head, 1996).

Baltis Vallis is by far the longest channel and is the most extensively studied for this reason. One area of interest is the topographic profile along its length. The first topographic profile along Baltis Vallis was achieved when it was still known as Hildr Fossa; 300 data points were taken along the length from the southern terminus to the northern terminus and show a general downward trend (Parker et al., 1992). With improved data, undulations were reported along the topographic profile and two long-wavelengths scales of deformation were observed, undulations in the order of hundreds as well as thousands of kilometers (Baker et al., 1997). These long-

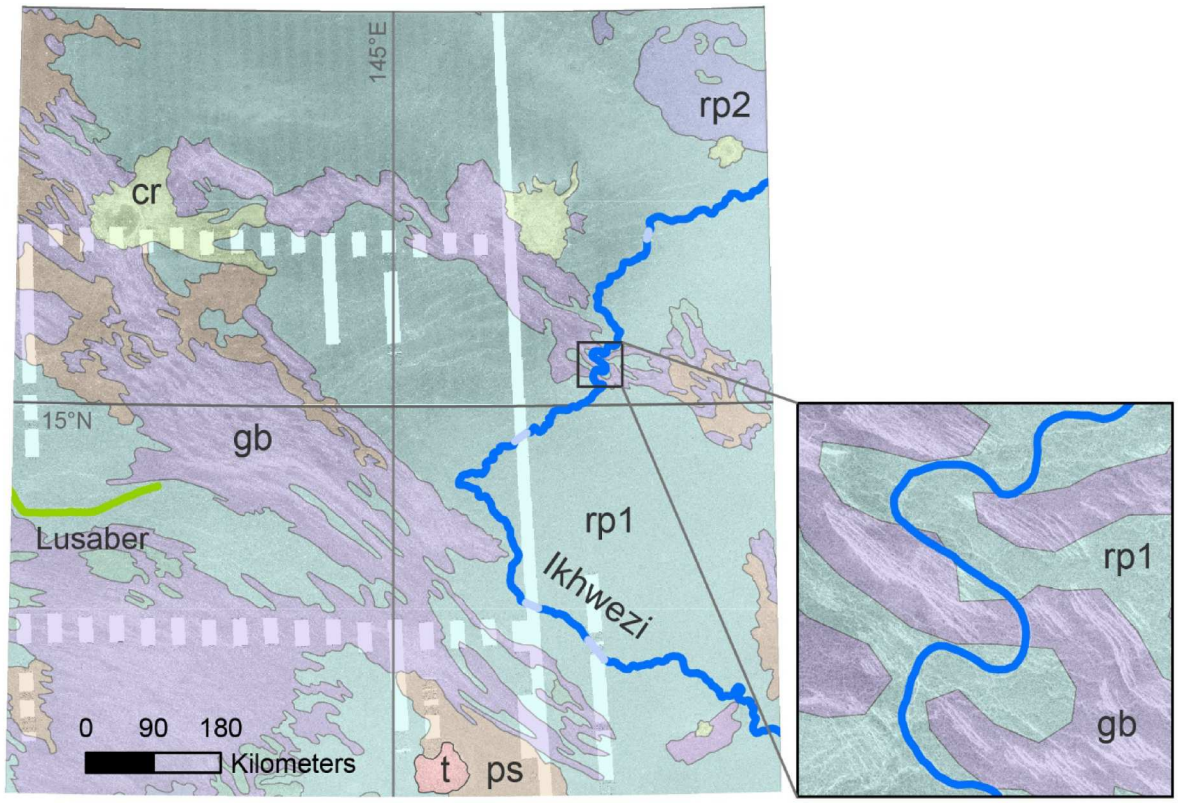

Figure 5. (a) The same example area as in Figure 1 showing Magellan SAR left-look mosaic overlain with the geologic map by Ivanov and Head (2011). Units are regional plains (rp1, rp2), groove belts (gb), smooth plains (ps), tesserae (t), and craters (cr). Note that Ikhwezi Vallis shows a pronounced sinuous path through a groove belt.

wavelength topographic changes were confirmed and further studied in later research (Conrad et al., 2021; Nimmo & McKenzie, 1998; Stewart & Head, 1999).

The deformation observed on the shorter length-scales at or below hundreds of kilometers is found to correspond to individual faults and faulted regions, while the long-wavelength topographic undulations on the order of thousands of kilometers is thought to be the result of subsurface dynamics (Conrad & Nimmo, 2023; Stewart & Head, 2000). Recent work used fourier transforms to constrain the wavelengths to ~225 and ~3,500 km (Conrad & Nimmo, 2023), whereby the longest wavelengths were hypothesized to be the result of dynamic uplift of the crust by mantle plumes. Because we produced a coherent dataset with consistent vertex spacing, future work studying topographic changes for all channels, such as those characterized for Baltis Vallis can make use of our map. Characterizations of the topography along channels will shed light into the long-wavelength topography and identify if they present along other channels, which, in turn, could be used to constrain the geophysical processes that formed them.

Software

Mapping and data collection were completed in ESRI ArcMap 10.8. Design of final map layout was performed in Adobe Illustrator 2024. RStudio 2023.09.0+463 was used to create the box-and-whisker plots.

Acknowledgements

We thank the editors Mike Smith and Monica Pondrelli for handling our paper. We also thank Prof. Mikhail Ivanov, Dr. Iván López, and Dr. Giedre Beconyte for their constructive and helpful reviews.

Disclosure statement

No potential conflict of interest was reported by the author(s).

Funding

SAB was supported by a research assistantship at the University of Georgia sponsored by Chevron Corporation.

Data availability statement

All data used in this mapping effort are publicly available. All image mosaics are located at: https://astrogeology.usgs.gov/search/map/venus_magellan_sar_fmap_left_look_global_mosaic_75m and https://astrogeology.usgs.gov/search/map/Venus/Magellan/Venus_Magellan_RightLook_mosaic_global_75m. The data that supports the findings of this study are openly available in Mendeley at https://doi.org/10.17632/frsh4z5f4v.1.

References

Baker, V. R., Komatsu, G., Gulick, V. C., & Parker, T. J. (1997). Channels and valleys. In S. W. Bougher, D. M. Hunten, & R. J. Phillips (Eds.), *Venus II: Geology, geophysics, atmosphere, and solar wind environment* (pp. 757–793). University of Arizona Press.

Baker, V. R., Komatsu, G., Parker, T. J., Gulick, V. C., Kargel, J. S., & Lewis, J. S. (1992). Channels and valleys on Venus: Preliminary analysis of Magellan data. *Journal of Geophysical Research: Planets*, *97*, 13421–13444. https://doi.org/10.1029/92je00927

Basilevsky, A. T., & Head, J. W. (1996). Evidence for rapid and widespread emplacement of volcanic plains on Venus: Stratigraphic studies in the Baltis Vallis Region. *Geophysical Research Letters*, *23*, 1497–1500. https://doi.org/10.1029/96gl00975

Basilevsky, A. T., & Head, J. W. (2003). The surface of Venus. *Reports on Progress in Physics*, *66*, 1699–1734. https://doi.org/10.1088/0034-4885/66/10/r04

Bledsoe, S. A., & Klimczak, C. (2024). *Global distribution of Lava channels on Venus*. Mendeley Data. https://doi.org/10.17632/frsh4z5f4v.1

Bray, V. J., Bussey, D. B. J., Ghail, R. C., Jones, A. P., & Pickering, K. T. (2007). Meander geometry of Venusian canali: Constraints on flow regime and formation time. *Journal of Geophysical Research: Planets*, *112*, 1–13. https://doi.org/10.1029/2006je002785

Bussey, D. B. J., Sørensen, S-A, & Guest, J. E. (1995). Factors influencing the capability of lava to erode its substrate: Application to Venus. *Journal of Geophysical Research: Planets*, *100*, 16941–16948. https://doi.org/10.1029/95je00894

Byrne, P. K., Klimczak, C., Williams, D. A., Hurwitz, D. M., Solomon, S. C., Head, J. W., Preusker, F., & Oberst, J. (2013). An assemblage of lava flow features on mercury. *Journal of Geophysical Research: Planets*, *118*, 1303–1322. https://doi.org/10.1002/jgre.20052

Conrad, J. W., & Nimmo, F. (2023). Constraining characteristic morphological wavelengths for Venus using Baltis Vallis. *Geophysical Research Letters*, *50*, 1–9. https://doi.org/10.1029/2022gl101268

Conrad, J. W., Nimmo, F., & Black, B. A. (2021, March 15–19). *Uplift record of Baltis Vallis, Venus*. 52nd Lunar and Planetary Science Conference, Lunar and Planetary Institute.

Dietterich, H. R., & Cashman, K. V. (2014). Channel networks within lava flows: Formation, evolution, and implications for flow behavior. *Journal of Geophysical Research: Earth Surface*, *119*, 1704–1724. https://doi.org/10.1002/2014jf003103

Ford, J. P., Plaut, J. J., Weitz, C. M., Farr, T. G., Senske, D. A., Stofan, E. R., Michaels, G., & Parker, T. J. (1993). *Guide to Magellan image interpretation*. National Aeronautics and Space Administration, Jet Propulsion Laboratory.

Gregg, T. K. P., & Greeley, R. (1993). Formation of Venusian Canali: Considerations of lava types and their thermal behaviors. *Journal of Geophysical Research: Planets*, *98*, 10873–10882. https://doi.org/10.1029/93je00692

Group, M. C. W. (1983). Channels and valleys on Mars. *GSA Bulletin*, *94*, 1035–1054. https://doi.org/10.1130/0016-7606(1983)94<1035:cavom>2.0.co;2

Head, J. W., Crumpler, L. S., Aubele, J. C., Guest, J. E., & Saunders, R. S. (1992). Venus volcanism: Classification of volcanic features and structures, associations, and global distribution from Magellan data. *Journal of Geophysical Research: Planets*, *97*, 13153–13197. https://doi.org/10.1029/92je01273

Hopper, J. P., & Leverington, D. W. (2014). Formation of Hrad Vallis (Mars) by low viscosity lava flows. *Geomorphology*, *207*, 96–113. https://doi.org/10.1016/j.geomorph.2013.10.029

Hurwitz, D. M., Head, J. W., Byrne, P. K., Xiao, Z., Solomon, S. C., Zuber, M. T., Smith, D. E., & Neumann, G. A. (2013a). Investigating the origin of candidate lava channels on Mercury with MESSENGER data: Theory and observations. *Journal of Geophysical Research: Planets*, *118*, 471–486. https://doi.org/10.1029/2012je004103

Hurwitz, D. M., Head, J. W., & Hiesinger, H. (2013b). Lunar sinuous rilles: Distribution, characteristics, and implications for their origin. *Planetary and Space Science*, *79*, 1–38. https://doi.org/10.1016/j.pss.2012.10.019

Hurwitz, D. M., Head, J. W., Wilson, L., & Hiesinger, H. (2012). Origin of lunar sinuous rilles: Modeling effects of gravity, surface slope, and lava composition on erosion rates during the formation of Rima Prinz. *Journal of Geophysical Research: Planets*, *117*, 1–15. https://doi.org/10.1029/2011je004000

IAU, USGS. (2012). Planetary nomenclature of Venus within KML and shapefile downloads [WWW Document]. Gazetteer of Planetary Nomenclature. Retrieved November 30, 2021, from https://planetarynames.wr.usgs.gov/GIS_Downloads

Ivanov, M. A., & Head, J. W. (2011). Global geological map of Venus. *Planetary and Space Science*, *59*, 1559–1600. https://doi.org/10.1016/j.pss.2011.07.008

Jaeger, W. L., Keszthelyi, L. P., McEwen, A. S., Dundas, C. M., & Russell, P. S. (2007). Athabasca Valles, Mars: A Lava-draped channel system. *Science*, *317*, 1709–1711. https://doi.org/10.1126/science.1143315

Jones, A. P., & Pickering, K. T. (2003). Evidence for aqueous fluid–sediment transport and erosional processes on Venus. *Journal of the Geological Society*, *160*, 319–327. https://doi.org/10.1144/0016-764902-111

Komatsu, G., Kargel, J. S., & Baker, V. R. (1992). Canali-type channels on Venus: Some genetic constraints. *Geophysical Research Letters*, *19*, 1415–1418. https://doi.org/10.1029/92gl01047

Lang, N. P., & Hansen, V. L. (2006). Venusian channel formation as a subsurface process. *Journal of Geophysical Research: Planets*, *111*, 1–15. https://doi.org/10.1029/2005je002629

Lang, N. P., & Hansen, V. L. (2010). Geologic map of the Greenaway quadrangle (V–24), Venus. U.S. Geological Survey Scientific Investigations Map 3089.

López, I., Martín, L., D'Incecco, P., Lang, N. P., & Achille, G. D. (2023). Geology of the Imdr Regio area of Venus. *Journal of Maps*, *19*, 2253832. https://doi.org/10.1080/17445647.2023.2253832

Nimmo, F., & McKenzie, D. (1998). Volcanism and tectonics on Venus. *Annual Review of Earth and Planetary Sciences*, *26*, 23–51. https://doi.org/10.1146/annurev.earth.26.1.23

Oshigami, S., & Namiki, N. (2007). Cross-sectional profiles of Baltis Vallis channel on Venus: Reconstructions from Magellan SAR brightness data. *Icarus*, *190*, 1–14. https://doi.org/10.1016/j.icarus.2007.03.011

Parker, T. J., Komatsu, G., & Baker, V. R. (1992). Longitudinal topographic profiles of very long channels in Venusian plains regions. In *Lunar and Planetary Science Conference XXIII* (pp. 1035–1036). Lunar and Planetary Institute.

Phillips, R. J., Raubertas, R. F., Arvidson, R. E., Sarkar, I. C., Herrick, R. R., Izenberg, N., & Grimm, R. E. (1992). Impact craters and Venus resurfacing history. *Journal of Geophysical Research: Planets*, *97*, 15923–15948. https://doi.org/10.1029/92je01696

Saunders, R. S., Spear, A. J., Allin, P. C., Austin, R. S., Berman, A. L., Chandlee, R. C., Clark, J., Decharon, A. V., Jong, E. M. D., Griffith, D. G., Gunn, J. M., Hensley, S., Johnson, W. T. K., Kirby, C. E., Leung, K. S., Lyons, D. T., Michaels, G. A., Miller, J., Morris, R. B., … Wall, S. D. (1992). Magellan mission summary. *Journal of Geophysical Research: Planets*, *97*, 13067–13090. https://doi.org/10.1029/92je01397

Schaber, G. G., Strom, R. G., Moore, H. J., Soderblom, L. A., Kirk, R. L., Chadwick, D. J., Dawson, D. D., Gaddis, L. R., Boyce, J. M., & Russell, J. (1992). Geology and distribution of impact craters on Venus: What are they telling us? *Journal of Geophysical Research: Planets*, *97*, 13257–13301. https://doi.org/10.1029/92je01246

Smrekar, S. E., Stofan, E. R., Mueller, N., Treiman, A., Elkins-Tanton, L., Helbert, J., Piccioni, G., & Drossart, P. (2010). Recent hotspot volcanism on Venus from VIRTIS emissivity data. *Science*, *328*, 605–608. https://doi.org/10.1126/science.1186785

Stewart, E. M., & Head, J. W. (1999, March 15–19). *Stratigraphic relations and regional slopes in the Baltis Vallis region, Venus: Implications for the evolution of topography*. Lunar and Planetary Science Conference XXX, Lunar and Planetary Institute.

Stewart, E. M., & Head, J. W. (2000, March 13–17). *Evidence for temporal continuity of deformation in the Baltis Vallis region of Venus from observations of canali topography*. Lunar and Planetary Science Conference XXXI. Presented at the Lunar and Planetary Science Conference XXXI, Lunar and Planetary Institute.

Strom, R. G., Schaber, G. G., & Dawson, D. D. (1994). The global resurfacing of Venus. *Journal of Geophysical Research: Planets*, *99*, 10899–10926. https://doi.org/10.1029/94je00388

Turcotte, D. L. (1993). An episodic hypothesis for Venusian tectonics. *Journal of Geophysical Research: Planets*, *98*, 17061–17068. https://doi.org/10.1029/93je01775

Williams-Jones, G., Williams-Jones, A. E., & Stix, J. (1998). The nature and origin of Venusian canali. *Journal of Geophysical Research: Planets*, *103*, 8545–8555. https://doi.org/10.1029/98je00243